doi: 10.1111/j.1365-3121.2008.00808.x

Alteration geochemistry of the Nopal I uranium deposit (Sierra Peña Blanca, Mexico), a natural analogue for a radioactive waste repository in volcanic tuffs

Georges Calas,[1] Pierre Agrinier,[2] Thierry Allard[1] and Philippe Ildefonse[1,†]

[1]*Institut de Minéralogie et de Physique des Milieux Condensés, Université Paris 6, Université Paris 7, Institut de Physique du Globe de Paris, CNRS, 140 rue de Lourmel, 75015 Paris, France;* [2]*Laboratoire de Géochimie des Isotopes Stables, Institut de Physique du Globe de Paris, Université Paris 7, CNRS, 2, place Jussieu, 75251 Paris Cedex 05, France*

ABSTRACT

Natural analogues provide an approach to characterize and test the long-term modelling of a repository performance. This article presents geochemical information about the alteration conditions of the Nopal I uranium deposit, Mexico, an analogue for the proposed Yucca Mountain radioactive waste repository. Mineralization and hydrothermal alteration of volcanic tuffs are contemporaneous, according to petrographic observations. Trace element geochemistry (U, Th, REE) provides evidence for local mobilization of uranium under oxidizing conditions and further precipitation under reducing conditions. O- and H-isotope geochemistry of kaolinite, smectite, opal and calcite suggests that argillic alteration proceeded at shallow depth with meteoric water at 25–75 °C, a low-temperature context, unusual for volcanic-hosted uranium deposits. This temperature range is compatible with some post-closure evolution models of the proposed Yucca Mountain repository.

Terra Nova, 20, 206–212, 2008

Introduction and geological context

The study of analogous natural systems provides an approach to characterize processes over geological time and to test the long-term predictive modelling of a repository performance (Petit, 1990; Murphy, 2000). The volcanic-hosted uranium deposit of Nopal I (Sierra Peña Blanca, Chihuahua, Mexico: Fig. 1) is probably the best-suited analogue for the proposed high-level nuclear waste repository at Yucca Mountain, Nevada. Both sites are located in semi-arid regions, in Tertiary rhyolitic ash flow tuffs overlying carbonate rocks in a basin and range context, within an unsaturated zone. The oxidation of the uraninite of Nopal I suggested phases likely to form during long-term alteration of spent fuel in a Yucca Mountain repository (Ildefonse *et al.*, 1990; Muller *et al.*, 1990; Pearcy *et al.*, 1994, 1995; Prikryl *et al.*, 1997).

Correspondence: G. Calas, Institut de Minéralogie et de Physique des Milieux, Condensés, Université Paris 6, Université Paris 7, Institut de Physique du Globe de Paris, CNRS, 140 rue de Lourmel, 75015 Paris, France. Tel.: +33 1 44276872; fax: +33 1 44273785; e-mail: calas@impmc.jussieu.fr

†Deceased.

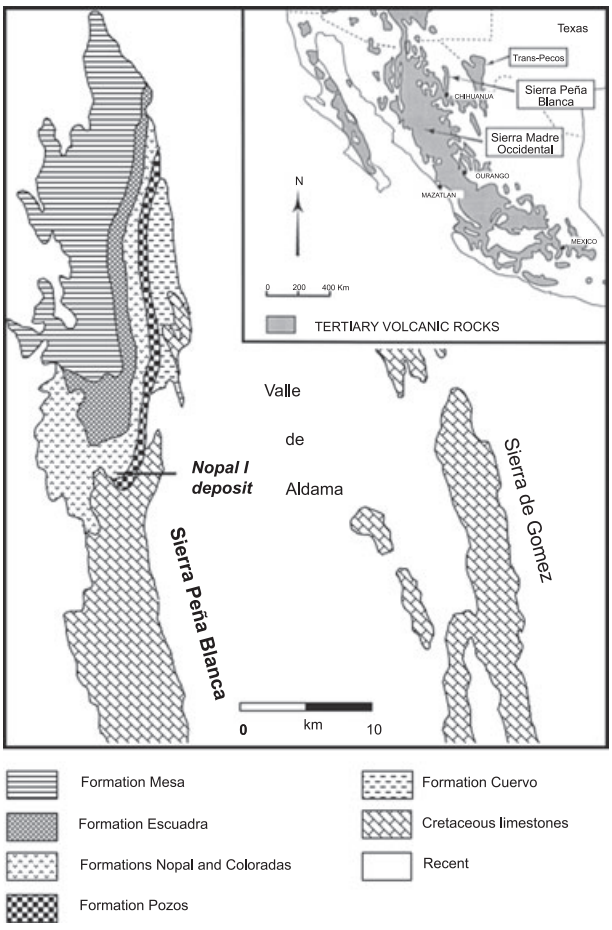

Fig. 1 Geological setting of the Nopal 1 uranium deposit in the Sierra Peña Blanca, Chihuahua, Mexico. The inset represents the location of the Sierra Peña Blanca on the eastern side of the Sierra Madre Occidental (after Calas, 1977).

In the Sierra Peña Blanca, rhyolitic tuffs (35–44 Ma: Alba and Chavez, 1974) overlie the Pozos conglomerate (53 Ma) and Cretaceous limestones (Calas, 1977; Goodell, 1981), as confirmed by an extensive drilling programme (Dobson *et al.*, 2005). The Nopal I uranium deposit occurs in the Nopal and Coloradas rhyolitic Formations, and is comprised of welded ash-flow tuffs (44 Ma) and weakly welded, lithic rich ash-flow tuffs respectively (Fig. 2). These tuffs are extensively altered with spatial zonation: kaolinite with late, minor halloysite is predominant inside the breccia pipe and late montmorillonite outside (Muller *et al.*, 1990). Kaolinite may occur in feldspar pseudomorphs or fracture fillings. When smectite and kaolinite coexist, smectite tactoids cover kaolinite plates and post-date them. The uranium mineralization associated with this alteration consists of residual uraninite within a breccia pipe, with an isotopic age of 32 Ma (Fayek *et al.*, 2006), and secondary U-minerals resulting from uraninite oxidation. Uraninite formation and hydrothermal argillization are contemporaneous, but oxidized mineralization is later than kaolinite fissure fillings that it recovers or crosscuts (Fig. 3). Migration of radionuclides since deposit formation was traced by structural defects caused in kaolinites by radioactivity (Ildefonse *et al.*, 1990; Muller *et al.*, 1990; Calas *et al.*, 2004).

Ore genesis models favour uraninite formation under hydrothermal conditions, contemporaneous with or after the main volcanic events (Calas, 1977; Cardenas-Flores, 1985; George-Aniel *et al.*, 1991; Pearcy *et al.*, 1994) with possible reactivation by a local geothermal system (Goodell, 1985). Temperatures of 200–250 °C from fluid inclusions (Aniel and Leroy, 1985) were recently contradicted by isotope-derived temperatures on uraninite: 45–55 °C and 10–20 °C for the main ore body and Pozos Formation respectively (Fayek *et al.*, 2006). The geochemical information presented here indicates an argillic alteration by meteoric fluids at low temperature (20–50 °C) under oxidizing conditions, which mobilized uranium prior to further reduction in the Nopal I pipe. These temperatures correspond to post-closure conditions predicted for the radioactive waste repository at Yucca Mountain.

Sampling and analytical methods

Sampling strategy was detailed in previous publications on Nopal kaolinites (Ildefonse *et al.*, 1990; Muller *et al.*, 1990). In addition to the breccia pipe, we investigated the upper and lower levels subjected to argillaceous alteration, representing the Nopal and Coloradas formations respectively. The open pit was sampled on level +10m along a SW transect, 75 m long (A samples). Samples were also collected on level 0 along two transects parallel to the rim and crosscutting the pipe (B and C samples respectively). Vertical profiles (D and E samples) were sampled outside the mineralized pipe, north of level 0. Late opal (Cesbron *et al.*, 1992) was sampled in the breccia pipe. Across Coloradas tuffs, we handpicked calcite in subvertical fractures in the −70m level (N-70–5), coatings on clayey aggregates (N-E22) and sub-horizontal fractures (N-D13). Calcite was also sampled in sub-horizontal fractures within Nopal rhyolite (N-B4).

Clay minerals were isolated (< 2 μm fractions) by the technique of sedimentation and centrifugation. Major and trace elements were determined by ICP-AES (JY 48 P spectrometer) at CRPG (Nancy, France). Oxygen isotope compositions were measured by the BrF_5 technique of Clayton and Mayeda (1963). Water was extracted by pyrolysis of solid samples at 1200 °C and then converted to hydrogen by reduction on zinc at 450 °C (Coleman *et al.*, 1982). CO_2 was obtained from $CaCO_3$ by H_3PO_4 attack at 25 °C (McCrea, 1950). Isotopic analyses were made using conventional isotope-ratio mass spectrometry and reported using the δ notation in units of per mil relative to SMOW for oxygen and hydrogen and relative to PDB for carbon. Analytical uncertainties are 3‰ (1σ) for δD, less than 0.3‰ (1σ) for $\delta^{18}O$ of silicates and better than 0.1‰ (1σ) for $\delta^{18}O$ and $\delta^{13}C$ of carbonates.

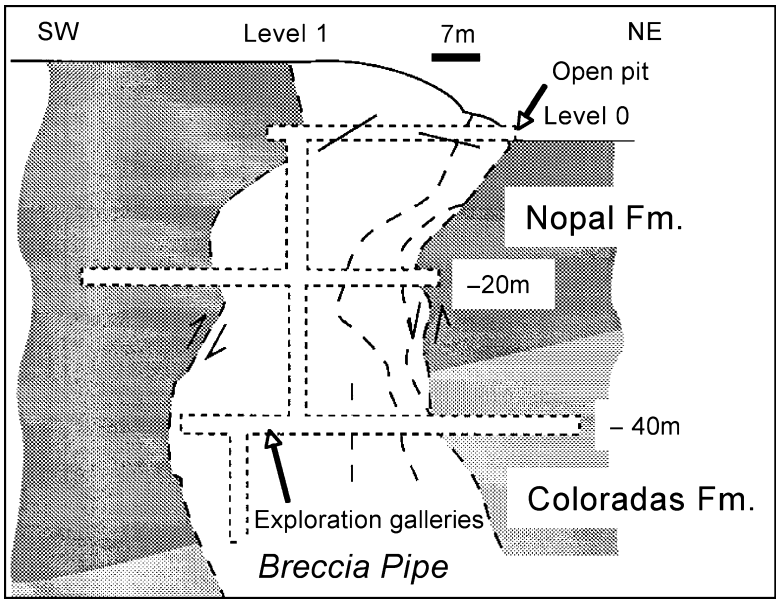

Fig. 2 Vertical section of the breccia pipe of the Nopal I deposit (after Ildefonse *et al.*, 1990).

Results

Geochemical changes during alteration

Alteration is characterized by Na and K depletion inside the pipe, while only K is depleted in the upper argillaceous layer (Tables 1 and 2). K-bearing secondary U-minerals within the depleted pipe confirm K mobility and availability during argillaceous alteration (Muller *et al.*, 1990; Pearcy *et al.*, 1995). Mg is enriched in smectite-bearing samples and Ca increases in the lower argillaceous layer, in relation to the presence of calcite.

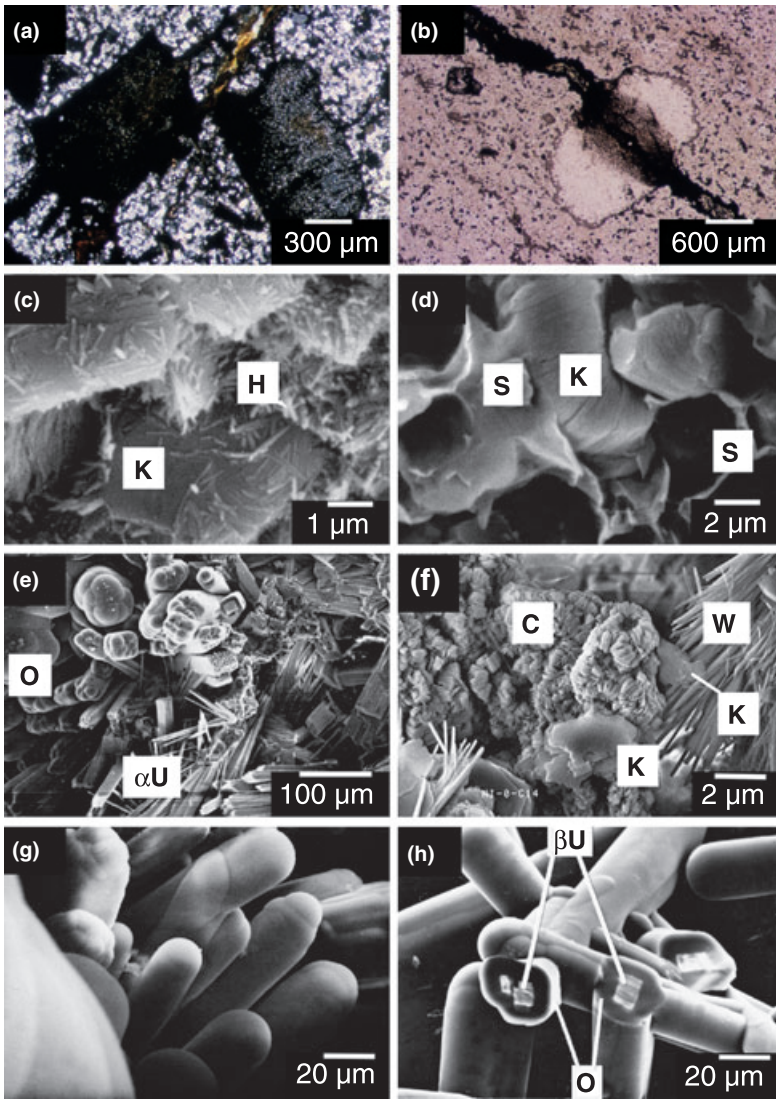

Fig. 3 Mineralogical parageneses showing the alteration minerals and their association with uranium mineralization in the Nopal I deposit. (a) Photomicrograph showing the intimate association between kaolinite and uraninite in a feldspar pseudomorph from level 0 gallery. The groundmass of the altered rhyolitic tuff consists mainly of secondary quartz. (b) Photomicrograph of a fissure filled with uraninite and minor kaolinite crossing a feldspar pseudomorph filled with kaolinite, from level 0 gallery. (c) SEM micrograph of a sample from the centre of the pipe showing kaolinite flakes (K) covered with elongated halloysite particles (H). (d) Kaolinite from the breccia pipe, usually found as tightly packed flakes (K), a typical habit for hydrothermal crystallization. Smectite (S) occurs as tactoids and crumpled films, which cover kaolinite crystals and post-date them. (e) Sample from the open pit, showing the association between opal (O) and α-uranophane (α-U: $Ca(UO_2)_2(SiO_3OH)_2.5H_2O$). (f) Kaolinite (K) from the level 0 gallery, associated with secondary uranyl minerals: weeksite (W: $K_2(UO_2)_2Si_6O_{15}.4H_2O$) and carnotite (C: $K_2(UO_2)_2(VO_4)_2{\cdot}3H_2O$). (g) Late opal deposition with a typical rod-shaped habit. (h) Broken rod-shaped opal (O) from the open pit, showing the presence of β-uranophane (βU) at the centre of the rod, explaining the typical habit of this late opal.

The Nopal and Coloradas rhyolitic tuffs have distinctive U, Th and REE contents (Magonthier, 1987). During alteration, Th concentration remains in the 37–55 p.p.m. and 12–18 p.p.m. ranges in the Nopal and Coloradas formations respectively (Tables 1 and 2). This confirms that Th behaves as an immobile element during alteration, as shown in mass balance studies of

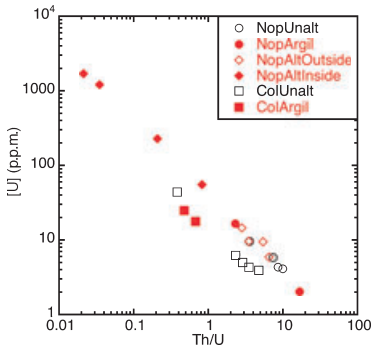

Fig. 4 Uranium and thorium variation among Peña Blanca samples (whole rock analysis). The samples come from the Nopal formations (NopUnalt: unaltered; NopArgil: argillaceously altered; NopAltOutside: altered outside the pipe; NopAltInside: altered inside the pipe) and Coloradas (ColUnalt: unaltered samples; ColArgil: argillaceously altered).

lateritic soils (Braun *et al.*, 1993). All samples retain the distinct Th/U ratio trend of the parent rock during uranium enrichment (Fig. 4), which confirms that the upper and lower parts of the argillic layer can be assigned to the Nopal and Coloradas formations, respectively.

REE patterns of fissure filling kaolinites are similar to those of the Nopal rhyolitic ash-flows (Magonthier, 1987) with a slight enrichment in light REE. In contrast, there is a clear distinction between kaolinite pseudomorphs after feldspars outside and inside the breccia pipe (Fig. 5). The former show a positive Ce anomaly, indicating oxidizing conditions (Braun *et al.*, 1990). The latter are characterized by a negative Eu anomaly, indicating reducing conditions, consistent with a pyrite-uraninite paragenesis (Calas, 1977; Aniel and Leroy, 1985). Oxidizing conditions outside the breccia pipe and in the argillaceous zone explain the variability of U concentration resulting from uranium leaching during rock alteration.

Stable isotope geochemistry

Kaolinites present similar average δD (−56‰) and $\delta^{18}O$ (15‰) values (Table 3). They plot within a restricted field that lies between the meteoric water line (MWL) and the weathering kaolinite line (KL). The gap (5‰ in $\delta^{18}O$ values) between the Nopal kaolinites and KL indicates

Table 1 Chemical composition of rock samples from the Nopal Formation (LOI = Loss of ignition). NI-C represents unaltered rocks outside of the mineralized area. Altered rocks have been sampled inside (N-A1 and N-A6) or outside (N-A9 and N-A17) the breccia pipe, and within the upper argillized tuff (N-E9 and N-E10). The concentrations are given in wt% for the major components and in p.p.m. for U and Th.

Samples	NI-C	N-A1	N-A6	N-A9	N-A17	N-E9	N-E10
SiO_2	74.28	78.95	58.89	75.99	75.07	65.37	62.52
Al_2O_3	12.38	12.78	14.73	12.69	12	12.86	14.49
TiO_2	0.24	0.25	0.16	0.25	0.22	0.25	0.28
Fe_2O_3	1.5	0.68	16.54	0.98	1.62	3.62	2.54
MnO	0.03				0.03	0.04	
MgO	0.11	0.03	0.06	0.03	0.04	1.45	1.85
CaO	0.28	0.11	0.13	0.08	0.32	1.61	1.67
Na_2O	1.58	0.08	0.03	0.4	0.64	1.64	1.48
K_2O	7.66	1.79	0.6	6.35	6.85	1.31	1.33
P_2O_5	0.14	0.15	0.17	0.12	0.14	0.16	0.15
LOI	1.59	4.73	8.85	2.64	2.58	12.07	13.8
Total	99.79	99.55	100.06	99.53	99.51	100.38	99.81
U	4.32	1723.8	1231.2	2.05	5.94	2.05	16.83
Th	37.17	37	43.03	34.14	38.73	34.14	38.77

Table 2 Chemical composition of rock samples from the Coloradas Formation, outside of the mineralized area. N0 represents an unaltered rock outside the mineralized area. N-E21 and N-E22 were sampled within the argillized tuff.

Samples	N0	N-E21	N-E22
SiO_2	71.3	58.3	53.85
Al_2O_3	13.09	14.01	12.42
TiO_2	0.28	0.46	0.38
Fe_2O_3	1.92	0.97	3.79
MnO		0.01	0.11
MgO	0.61	3.07	2.06
CaO	0.86	2.91	6.78
Na_2O	2.71	0.48	0.52
K_2O	6.17	0.45	0.48
P_2O_5	0.09	0.2	0.45
LOI	2.75	18.92	18.96
Total	99.78	99.78	99.8
U	3.9	17.9	25.11
Th	18.6	12.14	12

hydrothermal formation (Fig. 6). Using the kaolinite/water fractionation factors for D and ^{18}O (Lambert and Epstein, 1980; Sheppard and Gilg, 1996), the isotopic composition of water in equilibrium with kaolinite has been calculated for temperatures from 200 to 50 °C. The fact that kaolinites have $\delta^{18}O$ ($\approx +15.5‰$) different from those of fresh feldspars, usually, $\delta^{18}O$ $< 11‰$ (Rumble *et al.*, 1986), confirms a high water/rock ratio during kaolinite formation. Such high W/R conditions are generally only compatible with low temperature processes where fluids are essentially derived from meteoric water (Taylor, 1974). For temperatures around 50 °C, the calculated isotopic composition ($\delta D \approx -27 \pm 10‰$ and $\delta^{18}O \approx -5 \pm 2‰$) plots on the

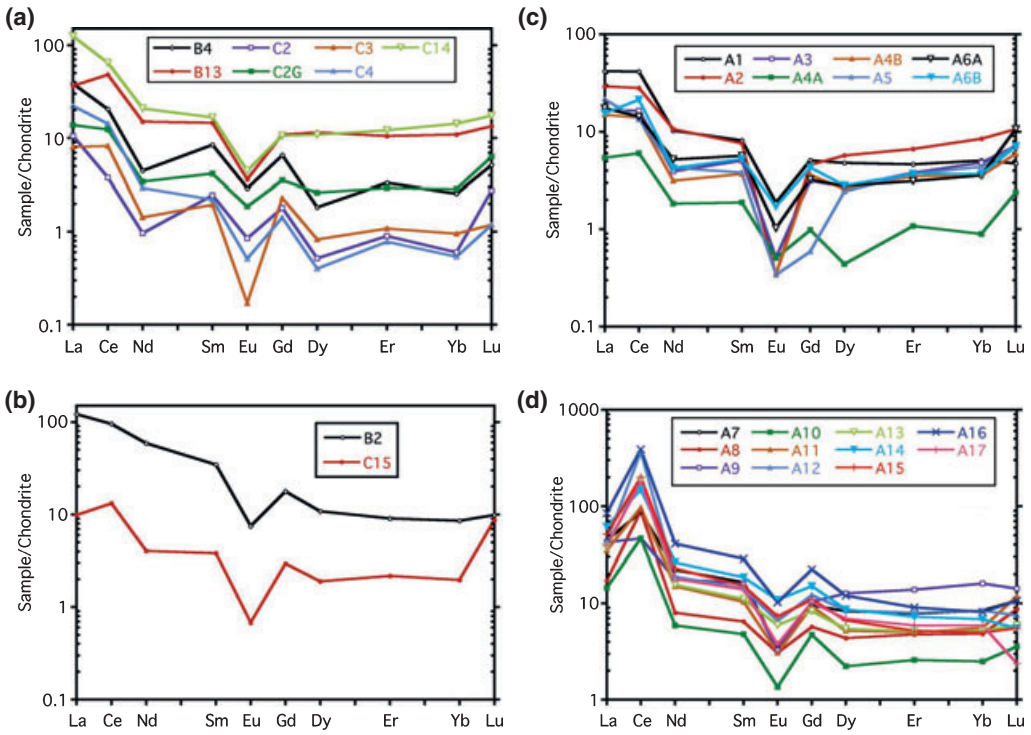

Fig. 5 Chondrite-normalized REE patterns of Nopal 1 kaolinites. (a) Fissure kaolinites from the pipe. (b) Fissure kaolinites from the barren rocks; there are no differences from the patterns shown in (a). (c) Kaolinite pseudomorphs after feldspar from the mineralized pipe. The absence of the Ce anomaly and the enhancement of the Eu anomaly indicate that alteration conditions were more reducing than in the barren rocks. (d) Kaolinite pseudomorphs after feldspar from barren volcanic rocks. The positive Ce anomaly indicates oxidizing alteration conditions of the volcanic rocks.

Table 3 δD, δ^{18}O and δ^{13}C isotope compositions of kaolinite, smectite, opal and calcite from the Nopal I deposit. The samples designated by * are outside the mineralized area.

Sample	Mineral	δD	$\delta^{18}O$	Associated minerals
N-A2	Kaolinite	−54	15.3	
N-A4A	Kaolinite	−58	15.1	
N-A17*	Kaolinite	−59	13.9	Smectite
N-B1*	Kaolinite	−58	15.4	
N-B13	Kaolinite	−53	16.2	Uranophane α
N-C2G	Kaolinite	−55	15.4	Uranophane β
N-C3	Kaolinite	−54	13.8	Weeksite
N-C14	Kaolinite	−56	15.1	Weeksite
N-C15	Kaolinite	−60	15.4	
N-D18*	Smectite	−53	18.3	
N-E16*	Smectite	−54	18.0	
N-E21*	Smectite	−52	19.7	
N-C4C	Opal		26.3	
N-C24	Opal		27.3	
NISSU	Opal		26.2	
		$\delta^{18}O$	$\delta^{13}C$	
N-B4*	Black calcite	29.5	−0.96	
N-D13*	Calcite coating	29.8	−3.42	
N-E22*	Calcite coating	31.6	−6.20	
NI-70-5*	White calcite	31.3	1.91	

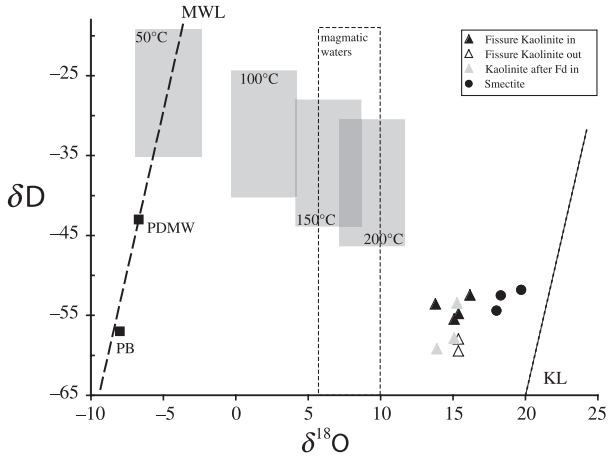

Fig. 6 δD–δ^{18}O plot of kaolinite and smectite from the Nopal deposit. Magmatic water field (dashed contour) is taken from Taylor (1974). KL stands for kaolinite line (Sheppard and Gilg, 1996); PDMW square is the locus of mean present day meteoric waters (Dobson *et al.*, unpublished data); PB square is the locus of the Nopal well waters (Dobson *et al.*, unpublished data). Small grey rectangular areas with temperature labels (50, 100, 150 and 200 °C) are the calculated isotopic compositions of water in equilibrium with the kaolinite (see text). Fissure kaolinite in = Fissure kaolinite from the pipe. Fissure kaolinite out = Fissure kaolinite from the barren rocks. Kaolinite after Fd in = Kaolinite pseudomorph after feldspar from the mineralized pipe.

MWL. The calculated temperature values are robust, as a δ^{18}O change of 2‰ in the isotopic composition of the fluid would change the inferred temperatures by less than 20 °C.

It is worth noting that the maximum potential kaolinization temperature is less than 200 °C, i.e. it is obtained when the calculated fluid δ^{18}O values matches the δ^{18}O of pristine magmatic waters (6 and 10‰; Taylor, 1974). But such a kaolinization temperature is highly unlikely as it is difficult to reconcile such a low temperature (≤200 °C, compared with magmatic temperatures ≥750 °C) with pristine magmatic waters preserved from mixing with the surrounding meteoric hydrothermal waters.

From the current knowledge of isotope fractionation factors, at least 10‰ for δD and more than 1‰ for δ^{18}O, inferred compositions for waters in equilibrium with the Nopal kaolinites match present-day local meteoric waters (PDMW: $\delta D \approx -43$‰ and $\delta^{18}O \approx -6.7$‰; International Atomic Energy Agency, 2004) but differ slightly from present-day Nopal well waters (PB: $\delta D \approx -57$‰ and $\delta^{18}O \approx -8$‰; Dobson *et al.*, in preparation). Similar inconsistencies have been noticed for kaolinites (Lombardi and Sheppard, 1977; Simeone *et al.*, 2005) and were attributed to a lack of knowledge of D/H fractionation between kaolinite and water for temperatures lower than 100 °C.

Smectite samples are slightly richer in D and ^{18}O (≈−56‰ and 17‰ respectively) than kaolinites (Table 3). The water isotopic composition calculated from smectite/water fractionation factors (Yeh and Epstein, 1978; Yeh, 1980) suggests formation in meteoric waters ($\delta D \approx -15 \pm 10$‰ and $\delta^{18}O \approx -3.5 \pm 2$‰) at around 40 °C (Fig. 6). The opal samples are richer in ^{18}O (≈26‰) than kaolinite and smectite (Table 3). Assuming a meteoric fluid ($\delta^{18}O \approx -5$ to −3.5‰), this implies that opal formed at around 30 °C, using the fractionation values of Kita *et al.* (1985).

The δ^{18}O values of calcites are homogeneous ($\approx 30.5 \pm 1$‰) and correspond to a low temperature (≤ 20 °C), assuming calcite precipitated from a meteoric fluid ($\delta^{18}O = -5$‰). The distribution of δ^{13}C values in the calcites indicates variability in the dissolved inorganic carbon pool (Deines *et al.*, 1974; Mook *et al.*, 1974). The δ^{13}C values are compatible with massive precipitation of carbonates in the high pH conditions of the argillaceous alteration zone, leading to a progressive decrease in the ^{13}C stock.

Discussion and conclusion

Evidence for hydrothermal alteration at low temperature

As the kaolinite is contemporaneous with the uraninite (Calas, 1977; Muller *et al.*, 1990), temperatures derived from isotopic data on kaolinite corre-

spond to primary mineralization. Fluid inclusion studies indicated temperatures of 250–200 °C for the uraninite–kaolinite association and 150 °C for late alteration and opal deposition (Aniel and Leroy, 1985). Fluid inclusions were investigated in rhyolitic and vapour phase quartz phenocrysts and not in the quartz formed during kaolinization, providing temperatures relevant to early events, ash-flow cooling or other post-volcanic processes. The origin of the discrepancy in the temperatures derived from fluid inclusions of opal is less clear.

Homogeneous δD values indicate high water/rock ratios. According to the O isotope data, kaolinites associated with the reduced mineralization formed at 75–50 °C, consistent with an epithermal system with meteoric fluids being recycled at shallow depth (Taylor, 1974). There is no constraint on the oxidized mineralization, subsequent to the kaolinite fissure fillings that it covers or cross-cuts. Eventually, smectite and opal crystallized at 20–45 °C, during fluid cooling or weathering conditions. Decreasing formation temperatures, from kaolinite to smectite and opal, confirm petrologic observations (Muller *et al.*, 1990). Our data are also consistent with $\delta^{18}O$-derived precipitation temperatures of 45–55 °C and 10–20 °C for the uraninite from the ore body and Pozos conglomerate, respectively, assuming a formation in fluids of meteoric origin ($\delta^{18}O = -7‰$: Fayek *et al.*, 2006). Both mineralization and alteration occurred at low temperature.

Constraints on the formation of the mineralization

Low formation temperature and geochemical similarities with parent rhyolitic tuffs, together with isotopic evidence of meteoric water, favour a local uranium source. Volcanic glasses are a major potential source of disseminated uranium. This element occurs as U(V) and U(IV) in magmas (Calas, 1979), and hydration of volcanic glasses does not affect uranium mobility (Zielinski, 1982). In contrast, leaching a devitrified glass under oxidizing conditions results in oxidation to easily mobilized U(VI) (George-Aniel *et al.*, 1991). Oxidizing conditions, shown by the positive cerium anomaly, are only found outside the breccia pipe, giving rise to massive uranium mobilization. Uranium may have been then transported as fluoride complexes like at Marysvale, Utah (Cunningham *et al.*, 1998) and channelled by the fracture system, which generated the breccia pipe. The presence of carbonates in this pipe indicates contamination by underlying limestones, providing sedimentary sulphides and organic matter favouring reducing conditions and uraninite/pyrite precipitation. The redox contrast between outside and inside the pipe is confirmed by cerium and europium anomalies respectively.

In contrast to the Nopal I deposit, most volcanic-hosted uranium deposits formed at high temperature. Tertiary uranium mineralization at McDermitt, Oregon (Castor and Henry, 2000) resulted from hydrothermal activity at 200–330 °C. Uranium deposits in Marysvale, Utah, formed also near 200 °C, $\delta^{18}O\text{-}H_2O \approx -1.5$ and $\delta D\text{-}H_2O \approx -130‰$ (Cunningham *et al.*, 1998). Finally, in the largest uranium volcanic-hosted deposit, Streltsovka caldera, fluid inclusion studies indicate temperatures close to 250 °C (Philippot *et al.*, 2000).

Nopal I alteration and the post-closure conditions at Yucca Mountain

Heat generated by decaying high level radioactive waste buried in a geological site will substantially increase the temperature of repository rocks. Numerical simulations have been conducted on the response of the unsaturated zone system of Yucca Mountain repository to heat generated from the waste. With no ventilation, a thermal–hydrological (TH) model (Haukwa *et al.*, 2003) predicts the development of temperatures exceeding 100 °C above the potential repository for hundreds of years. In this case, boiling may occur even within the pillars and last up to 1000 years. Ventilation results in a cooler environment, with temperatures in the pillars predicted to rise to an average of 80–85 °C. With and without ventilation, the TH model predicts a temperature increase at the water table to an average of 60–65 °C. Similarly, a coupled thermal, hydrological and mechanical (THM) analysis (Rutqvist and Tsang, 2003) shows that the temperature in the rock mass away from the drift continues to rise after the forced ventilation period, with the mid-pillar temperature approaching 100 °C after 1000 years. Argillaceous alteration conditions at Nopal I indicate temperatures relevant to predictions of the post-closure thermal evolution of Yucca Mountain repository, based on TH and THM models.

Acknowledgements

The authors are indebted to the Mexican Federal Agencies in charge of uranium exploration, Consejo de Recursos Minerales, INEN and URAMEX, for their help in the fieldwork during three decades and in particular, help rendered by F.J. Altamirano, R. Chavez A., S. Constantino H., C.R. Villasana and R. Yza D. We thank Pat Dobson and Mostafa Fayek for fruitful discussions and information exchange. We acknowledge the support by the Commissariat à l'Energie Atomique-Direction de l'Approvisionnement en Matières Nucléaires. This is IPGP contribution 2355.

References

Alba, L.A. and Chavez, R., 1974. K-Ar ages from volcanic rocks from the Central Peña Blanca, Chihuahua, Mexico. *Isochron West.*, **10**, 21–23.

Aniel, B. and Leroy, J., 1985. The reduced uraniferous mineralizations associated with the volcanic rocks of the Sierra Peña Blanca (Chihuahua, Mexico). *Am. Mineral.*, **70**, 1290–1297.

Braun, J.J., Pagel, M., Muller, J.P., Bilong, P., Michard, A. and Guillet, B., 1990. Cerium anomalies in lateritic profiles. *Geochim. Cosmochim. Acta*, **54**, 781–795.

Braun, J.J., Pagel, M., Herbillon, A. and Rosin, C., 1993. Mobilization and redistribution of REE's and thorium in a syenitic lateritic profile. A mass balance study. *Geochim. Cosmochim. Acta*, **57**, 4419–4434.

Calas, G., 1977. Les phénomènes d'altération hydrothermale et leur relation avec les minéralisations uranifères en milieu volcanique: Le cas des ignimbrites tertiaires de la Sierra Peña Blanca, Chihuahua, Mexico. *Sci. Géol. Bull.*, **30**, 3–18.

Calas, G., 1979. Etude expérimentale du comportement de l'uranium dans les magmas: états d'oxydation et coordinance. *Geochim. Cosmochim. Acta*, **43**, 1521–1531.

Calas, G., Allard, T., Balan, E., Morin, G. and Sorieul, S., 2004. Radiation-induced defects in nonradioactive natural minerals: mineralogical and environmental

significance. *Mat. Res. Soc. Symp. Proc.*, **792**, 81–92.
Cardenas-Flores, D.F., 1985. Volcanic stratigraphy and U-Mo mineralization of the Sierra de Peña Blanca district, Chihuahua, Mexico. In: *Uranium Deposits in Volcanic Rocks* (IAEA, ed.). IAEA-TC-490/31. International Atomic Energy Agency, Vienna, 125–136.
Castor, S.B. and Henry, C. D., 2000. Geology, geochemistry, and origin of volcanic rock-hosted uranium deposits in northwestern Nevada and southeastern Oregon, USA. *Ore Geol. Rev.*, **16**, 1–40.
Cesbron, F., Ildefonse, P. and Sichere, M.C., 1992. New mineralogical data on uranophane and beta-uranophane; synthesis of uranophane. *Miner. Mag.*, **57**, 301–308.
Clayton, R.N. and Mayeda, T.K., 1963. The use of bromine pentafluoride in the extraction of oxygen from oxides and silicates for isotopic analysis. *Geochim. Cosmochim. Acta*, **27**, 43–52.
Coleman, M.L., Shepherd, T.J., Durham, J.J., Rouse, J.E. and Moore, G.R., 1982. Reduction of water with zinc for hydrogen isotope analysis. *Anal. Chem.*, **54**, 993–995.
Cunningham, C.G., Rasmussen, J.D., Steven, T.A., Rye, R.O., Rowley, D., Romberger, S.B. and Selverstone, J., 1998. Hydrothermal uranium deposits containing molybdenum and fluorite in the Marysvale volcanic field, west-central Utah. *Mineralium. Deposita*, **33**, 477–494.
Deines, P., Langmuir, D. and Harmon, R.S., 1974. Stable carbon isotope ratios and the existence of a gas phase in the evolution of carbonate ground waters. *Geochim. Cosmochim. Acta*, **38**, 1147–1164.
Dobson, P.F., Goodell, P.C., Fayek, M., Melchor, F., Murrell, M.T., Simmons, A., Reyes-Cortés, I.A., de la Garza, R. and Oliver, R.D., 2005. Stratigraphy of the PB-1 well, Nopal I uranium deposit, Sierra Peña Blanca, Chihuahua, Mexico. *Geol. Soc. Am. Abstr. Progr.*, **37**, 7–196.
Fayek, M., Ren, M., Goodell, P., Dobson, P., Saucedo, A.L., Kelts, A., Utsunomiya, S., Ewing, R.C., Riciputi, L.R. and Reyes, I., 2006, Paragenesis and geochronology of the Nopal I uranium deposit, Mexico. In: *Proceedings of the Eleventh International High-Level Radioactive Waste Management Conference, April 30-May 4, 2006, Las Vegas, NV*, pp. 55–62. American Nuclear Society, La Grange Park, IL.
George-Aniel, B., Leroy, J.L. and Poty, B., 1991. Volcanogenic uranium mineralization in the Sierra Pefia Blanca District, Chihuahua, Mexico: three genetic models. *Econ. Geol.*, **86**, 233–248.
Goodell, P.C., 1981. Geology of the Peña Blanca uranium deposits, Chihuahua, Mexico. In: *Uranium in Volcanic and Volcaniclastic Rocks* (P.C. Goodell and A.C. Waters, eds). *AAPG Studies Geol.*, **13**, 275–291.
Goodell, P.C., 1985, Chihuahua City uranium province, Chihuahua, Mexico. In: *Uranium Deposits in Volcanic Rocks* (IAEA, ed.). IAEA-TC-490/31. International Atomic Energy Agency, Vienna, 97–124.
Haukwa, C.B., Wu, Y.S. and Bodvarsson, G.S, 2003. Modeling thermal–hydrological response of the unsaturated zone at Yucca Mountain, Nevada, to thermal load at a potential repository. *J. Contaminant Hydrol.*, **62–63**, 529–552.
Ildefonse, Ph., Muller, J.P., Clozel, B. and Calas, G., 1990. Study of two alteration systems as natural analogues for radionuclide release and migration. *Eng. Geol.*, **29**, 413–439.
International Atomic Energy Agency, 2004. *Global Network of Isotopes, "Precipitation. The GNIP Database"* [WWW document]. http://www-naweb.iaea.org/napc/ih/GNIP/IHS-GNIP.html (last accessed April 2008).
Kita, I., Taguchi, S. and Matsubaya, O., 1985. Oxygen isotope fractionation between amorphous silica and water at 34–93°C. *Nature*, **314**, 83–84.
Lambert, S.J. and Epstein, S., 1980. Stable isotope investigations of an active geothermal in Valles Caldera, Jemez Mountains, New Mexico. *J. Volcanol. Geoth. Res.*, **8**, 111–129.
Lombardi, G. and Sheppard, S.M.F., 1977. Petrographic and isotopic studies of the altered acid volcanics of the Tolfa-Cerite area, Italy: the genesis of the clays. *Clay Miner.*, **12**, 147–162.
Magonthier, M.C., 1987. Relations entre les minéralisations d'uranium de la Sierra Peña Blanca (Mexique) et les ignimbrites porteuses. *Bull. Minéral.*, **110**, 305–317.
McCrea, J.M., 1950. On the isotopic chemistry of carbonates and a paleotemperature scale. *J. Chem. Phys.*, **18**, 849–857.
Mook, W.G., Bommerson, J.C. and Staverman, W.H., 1974. Carbon isotope fractionation between dissolved bicarbonate and gaseous carbon dioxide. *Earth Planet. Sci. Lett.*, **22**, 169–176.
Muller, J.P., Ildefonse, Ph. and Calas, G., 1990. Paramagnetic defect centers in hydrothermal kaolinite from an altered tuff, (Nopal uranium deposit, Chihuahua, Mexico). *Clays Clay Miner.*, **38**, 600–608.
Murphy, W.M., 2000. Natural analogs and performance assessment for geologic disposal of nuclear waste. *Mater. Res. Soc. Symp. Proc.*, **608**, 533–544.
Pearcy, E.C., Prikryl, J.D., Murphy, W.M. and Leslie, B.W., 1994. Alteration of uraninite from the Nopal I deposit, Peña Blanca district, Chihuahua, Mexico, compared to degradation of spent nuclear fuel in the proposed US high-level nuclear waste repository at Yucca Mountain, Nevada. *Appl. Geochem.*, **9**, 713–732.
Pearcy, E.C., Prikryl, J.D. and Leslie, B.W., 1995. Uranium transport through fractured silicic tuff and relative retention in areas with distinct fracture characteristics. *Appl. Geochem.*, **10**, 685–704.
Petit, J.C., 1990. Migration of radionuclides in the geosphere: what can we learn from natural analogs? *Radiochim. Acta*, **51**, 181–188.
Philippot, P., Menez, B., Simionovici, A., Chabiron, A., Cuney, M., Snigirev, A. and Snigireva, I., 2000. X-ray imaging of uranium in fluid inclusions. *Terra Nova*, **12**, 84–89.
Prikryl, J.D., Pickett, D.A., Murphy, W.M. and Pearcy, E.C, 1997. Migration behavior of naturally occurring radionuclides at the Nopal I uranium deposit, Chihuahua, Mexico. *J. Contaminant Hydrol.*, **26**, 61–69.
Rumble, D., Ferry, J.M. and Hoering, T.C., 1986. Oxygen isotope geochemistry of hydrothermally-altered synmetamorphic granitic rocks from South-Central Maine, USA. *Contrib. Mineral. Petr.*, **93**, 420–428.
Rutqvist, J. and Tsang, C.F., 2003. Analysis of thermal–hydrologic–mechanical behavior near an emplacement drift at Yucca Mountain. *J. Contaminant Hydrol.*, **62–63**, 637–652.
Sheppard, S.M.F. and Gilg, H.A., 1996. Stable isotope geochemistry of clay minerals. *Clay Miner.*, **31**, 1–24.
Simeone, R., Dilles, J.H., Padalino, G. and Palomba, M., 2005. Mineralogical and stable isotope studies of Kaolin deposits: shallow epithermal systems of western Sardinia, Italy. *Econ. Geol.*, **100**, 115–130.
Taylor, H.P., Jr, 1974. The application of oxygen and hydrogen isotope studies to problems of hydrothermal alteration and ore deposition. *Econ. Geol.*, **69**, 843–883.
Yeh, H.W., 1980. D/H ratios and late-stage dehydration of shales during burial. *Geochim. Cosmochim. Acta*, **44**, 341–352.
Yeh, H.W. and Epstein, S., 1978. Hydrogen isotope exchange between clay minerals and sea water. *Geochim. Cosmochim. Acta*, **42**, 140–143.
Zielinski, R.A., 1982. The mobility of uranium and other elements during alteration of rhyolite ash to montmorillonite: a case study in the Troublesome Formation, Colorado, U.S.A. *Chem. Geol.*, **35**, 185–204.

Received 9 July 2007; revised version accepted 25 March 2008

